

K -matrix analysis of the $^{12}\text{C}(\alpha, \gamma)$ reaction at low energy

B. W. Filippone, J. Humblet,* and K. Langanke†

W. K. Kellogg Radiation Laboratory, California Institute of Technology, Pasadena, California 91125

(Received 6 February 1989)

The most recent data for the $^{12}\text{C}(\alpha, \gamma)^{16}\text{O}$ reaction are parametrized in terms of a K matrix in order to derive the astrophysical $S(E)$ factor at stellar energies. This straightforward parametrization introduces neither boundary condition constants nor channel radii. To constrain the free parameters, all the available data for the phase shifts $\delta_l (l=1, 2)$ of $^{12}\text{C}(\alpha, \alpha)^{12}\text{C}$ were simultaneously fitted with those for the $E1$ and $E2$ radiative captures. For each of the three sets of capture data we have analyzed, χ^2 tests have been performed with different types of energy-dependent background terms, namely, polynomials and nonresonant echo poles (in the sense of McVoy). The introduction of such poles is motivated by the falling of the δ_l phase shift at higher energies. On the basis of the present analysis, it is concluded that, from the data available, one can derive an allowed range for $S(0.3)$, from 0.00 to 0.17 MeV b. No confidence can be given to a so-called best value of $S(0.3)$ within this range because such a value is dependent on both the data set analyzed and the type of background terms introduced into the parametrized K matrix.

I. INTRODUCTION

Several recent experimental¹⁻⁴ and theoretical⁵⁻⁸ studies have attempted to determine the cross section of the reaction $^{12}\text{C}(\alpha, \gamma)^{16}\text{O}$ at very low energies. They are motivated by the importance of this reaction in the nucleosynthesis taking place during the helium-burning stage of stellar evolution.⁹⁻¹¹ At the most effective stellar energy ($E_{\text{c.m.}} \approx 0.3$ MeV), the cross section is much too small to be measured directly. The corresponding astrophysical S factor is defined in terms of the cross section σ by

$$S(E) = E \exp(2\pi\eta) \sigma(E), \quad (1.1)$$

where η is the Sommerfeld parameter

$$(\eta = Z_1 Z_2 e^2 / hv = 3.273\,624 E^{-1/2})$$

and E the center-of-mass energy in MeV. The value of $S(E)$ at $E = 0.3$ MeV has been obtained by extrapolation from higher energy data and has been computed using various theoretical approaches.^{5-8, 12-14}

Prior to 1982, S factors at $E = 0.3$ MeV [$S(0.3)$] near 0.10 MeV b have been obtained and recommended for nucleosynthesis calculations.¹⁵ In particular, this value is in agreement with that derived from earlier Dyer and Barnes¹⁶ data for the $E1$ capture alone. In 1982, much higher values, near 0.40 MeV b, were obtained by Kettner *et al.*¹ for the combined $E1$ and $E2$ captures. Thereafter, general theoretical papers⁵⁻⁸ confirmed the importance of the $E2$ contribution to the $^{12}\text{C}(\alpha, \gamma)^{16}\text{O}$ rate at astrophysical energies and reported S factors in the range 0.23 to 0.36 MeV b. A value of 0.24 MeV b was subsequently recommended in the compilation of Caughlan *et al.*¹⁷ Still more recently, new experimental data²⁻⁴ and a revised parametrization¹² of older data suggest a smaller S factor closer to 0.20 MeV b, with, however, a wide range of possible values.

This situation results mainly from the lack of precision of part of the relevant experimental data, from the extreme difficulty to improve them,¹⁸⁻²¹ and from the need to extrapolate these data to much lower energies. This last point is, of course, of major importance. The exact parametrized cross sections deduced from a formal theory are impractical for comparison with experiment, and they must be simplified into formulas containing only a few free parameters. This can lead to different, non-equivalent approximations, while an *a priori* objective estimate of their intrinsic and relative value is often difficult, if not impossible. In an R -matrix parametrization, for example, when several levels are involved, the relation between the free parameters and the data is not simple. This has given rise to errors and misinterpretations in the analyses as pointed out recently by Barker¹² for the $^{13}\text{C}(\alpha, \gamma)$ reaction. As for the $S(E)$ factor recently computed by an entirely microscopic calculation,⁸ it agrees with the Redder *et al.*¹² data only when corrections are applied *a posteriori*.

In the present paper, we report the results we have obtained by fitting to a modified K -matrix parametrization all the best data presently available for $^{12}\text{C}(\alpha, \gamma)$ and $^{12}\text{C}(\alpha, \alpha)$. The modified K matrix \mathcal{H} was used by Humblet *et al.*²² in 1976, but with earlier data on the δ_1 phase shift, as explained in Secs. III and VI. This work also did not consider a possible $E2$ contribution to the $^{12}\text{C}(\alpha, \gamma)^{16}\text{O}$ rate, because of the lack of sufficient experimental data.

The \mathcal{H} -matrix parametrization is straightforward in its application, and it introduces only parameters which are independent of the channel radii, as is the collision matrix \mathcal{S} itself. The parameters associated with the resonances (resonance energies and reduced widths) are directly related to the data, since there is no energy shift, and no distinction has to be made between formal and observed widths. It is also well adapted to fit bound-state data; this is of particular importance in the present case

for both $E1$ and $E2$ captures. The part of the \mathcal{H} matrix corresponding to the observed resonances has a unique parametrized form, while its relation to the collision matrix is also unambiguously fixed and free of boundary condition constants. Because of the extrapolation to low energies, it is also important to note that for any few-level approximation of \mathcal{H} there corresponds an S matrix satisfying the unitarity condition.

Section II introduces the \mathcal{H} matrix and its parametrized form. Its two-level plus background approximations and the corresponding phase shift to be fitted to the data on $^{12}\text{C}(\alpha, \gamma)^{16}\text{O}$ and $^{12}\text{C}(\alpha, \alpha)^{12}\text{C}$ are given in Sec. III. To account for the decrease of the scattering phase shifts at high energies, "echo poles" (in the sense of McVoy^{23,24}) are introduced in the background terms. At the energy of such a pole, the scattering phase shift is *decreasing* through $\pi/2 \pmod{\pi}$. These poles are not related to resonances, but rather play a role similar to the hard-sphere scattering phase shift in an R -matrix parametrization. The results of the simultaneous parametrization of the $E1$ capture cross section and the phase shift δ_1 are given in Sec. IV. Fits are made successively to the $E1$ capture data of Dyer and Barnes,¹⁶ Redder *et al.*,² and the new Caltech⁴ data, each fitted together with the elastic scattering data of Clark *et al.*,²⁵ Jones *et al.*,²⁶ and Plaga *et al.*³ Similarly, in Sec. V, we obtain the simultaneous fit to the $E2$ capture data of Redder *et al.*² and the phase shift δ_2 obtained by Plaga *et al.*³ The results of the fit are discussed in Sec. VI, together with those obtained for an alternate choice of background terms corresponding to the nonresonant part of the elements of the \mathcal{H} matrix. The latter fits show that the best value of $S(0.3)$ depends very strongly on the analytical form given to the background terms. It is concluded that, at present, one can only obtain a *range* in which $S(0.3)$ is compatible with the data, rather than stressing a so-called "best value" of $S(0.3)$ corresponding to a χ^2 minimization and assigning some error to it.

II. THE MODIFIED K MATRIX

The \mathcal{H} matrix is a generalized collision matrix.^{22,27} Its relation to the conventional transition and collision matrices \mathcal{T} and \mathcal{S} , is

$$\mathcal{T} = 1 - \mathcal{S} = 2ip\mathcal{H}(1 + i\mu\mathcal{H})^{-1}p \quad (2.1)$$

in which p and μ are diagonal matrices. In terms of the Sommerfeld parameter η_c and the wave number k_c , the diagonal element p_c of p in channel c with angular momentum l for the relative motion, is defined as

$$p_c = \epsilon_l k_c^{l+1/2} \quad (2.2)$$

with

$$\epsilon_l(\eta_c) = \eta_c^l u_l(\eta_c)^{1/2} C_0(\eta_c) / l! ,$$

$$u_0 = 1, \quad u_l = (1 + l^2 \eta_c^{-2}) u_{l-1} ,$$

$$C_0(\eta_c) = [2\pi\eta_c / (e^{2\pi\eta_c} - 1)]^{1/2} ,$$

while the diagonal element μ_c of μ is²²

$$\mu_{c+} = p_c^2, \quad \mu_{c-} = 0 , \quad (2.3)$$

is an open (c^+) and closed (c^-) channel, respectively.²⁸

The \mathcal{H} matrix is a real symmetric matrix. It is defined by means of linear combinations of the conventional radial Coulomb wave functions F_l, G_l , namely²² \bar{F}_l, \bar{G}_l , which are entire functions²⁹ of the energy E , so that it has no singularities other than its poles. These poles are assumed to be simple, such that the element \mathcal{H}_{dc} can be given the parametrized form

$$\mathcal{H}_{dc} = \sum_{\lambda} \frac{g_{d\lambda} g_{c\lambda}}{E - E_{\lambda}} + B_{dc} . \quad (2.4)$$

The real parameters $E_{\lambda}, g_{c\lambda}, g_{d\lambda}$ are to be associated with an observed resonance, while the background term B_{dc} is potentially energy dependent; it includes contributions from the distant poles and any other nonresonant contribution to \mathcal{H}_{dc} . In particular, B_{dc} can contain echo poles, i.e., pole terms $g_{d\lambda} g_{c\lambda} / (E - E_{\lambda})$ in which both $g_{c\lambda}$ and $g_{d\lambda}$ are imaginary, so that in a diagonal element \mathcal{H}_{cc} the residue $g_{c\lambda}^2$ is negative. Such poles are not related to resonances.²⁴

The factorization of the residues $g_{d\lambda} g_{c\lambda}$ results from Green's theorem,²⁴ as in the R - and \mathcal{S} -matrix parametrizations. The partial and total widths associated with a resonance level E_{λ} are

$$\Gamma_{c\lambda} = 2p_c^2 g_{c\lambda}^2, \quad \Gamma_{\lambda} = \sum_{c^+} \Gamma_{c\lambda} . \quad (2.5)$$

Because $\text{Re}(i\mu_c) = 0$, there are no level shifts and the E_{λ} are the "observable" resonance energies.²² No distinction is made between formal and observed widths. Moreover, if E_{λ} is below the energy E_c of the threshold of channel c , i.e., $E_{c\lambda} = E_{\lambda} - E_c < 0$, this state satisfies a bound-state boundary condition in channel c .³⁰

In Eq. (2.5), for a photon channel, such as $^{16}\text{O} + \gamma$, one has

$$p_c^2 = p_{l\gamma}^2 = k_{\gamma}^{2l+1} \quad (2.6)$$

with $k_{\gamma} = (Q + E) / \hbar c$.

Before turning to the $^{12}\text{C}(\alpha, \gamma)$ reaction, it is important to clarify one aspect of the relationship between the R - and \mathcal{H} -matrix parametrizations. Recently, Barker¹² has suggested that a \mathcal{H} -matrix fit is essentially identical with an R -matrix fit with zero-channel radius. However, this is inconsistent with the definitions of the \mathcal{S} , R , and \mathcal{H} matrices and the relationships existing between them.

The threshold factors $\epsilon_l k^{l+1}, \epsilon_l^{-1} k^{-l}$ are defined in such a way that the limits, as $k \rightarrow 0$, of $F_l / \epsilon_l k^{l+1}$ and $G_l / \epsilon_l k^{-l}$ are finite and nonvanishing when $0 < r < \infty$. The same factors appear also in the limiting values of $r^{-l-1} F_l$ and $r^l G_l$ for $r \rightarrow 0$. For $r \approx 0$, one has indeed³¹

$$\begin{aligned} F_l &\approx r^{l+1} \epsilon_l k^{l+1} / (2l+1)!! , \\ G_l &\approx r^{-l-1} \epsilon_l^{-1} k^{-l} / (2l+1)!! / (2l+1) . \end{aligned} \quad (2.7)$$

But, when the latter properties are introduced into the relationship between the \mathcal{S} and R matrices, one obtains a relationship appreciably different from Eq. (2.1). More-

over, for a vanishing-channel radius, R reduces to a constant,³² \mathcal{S} reduces to unity, \mathcal{H} vanishes and there is no "internal region."

In the definition of the modified Coulomb wave functions \bar{F}_l, \bar{G}_l , and hence also of the \mathcal{H} matrix, the threshold factors have been isolated because of their analytical structure and their very strong energy dependence. Rather than being included in a function which is to be parametrized, the r -independent threshold factors $\epsilon_l k^{l+1}, \epsilon_l^{-1} k^{-l}$ are better and more easily isolated and treated exactly in a \mathcal{H} -matrix parametrization, without restricting the channel radius to small or vanishing values.

III. THE PARAMETRIZED CROSS SECTIONS

Since the ground states of ^4He , ^{12}C , and ^{16}O are 0^+ states, the observed $E1$ and $E2$ cross sections for $^{12}\text{C}(\alpha, \gamma)$ capture into the ground state of ^{16}O are given by

$$\sigma_{E1}(\alpha, \gamma) = (2l+1)\pi k_\alpha^{-2} |\mathcal{T}_{l\gamma\alpha}|^2, \quad (3.1)$$

where l ($=1$ or 2) is both the angular momentum of the relative motion in the entrance channel and the multipolarity of the emitted γ radiation in the exit channel, while the indices α, γ correspond respectively to the channels $^{12}\text{C} + \alpha$ and $^{16}\text{O} + \gamma$.

The inversion of the 2×2 matrices implied by Eq. (2.1) is easily performed exactly. However, since the fluxes in the γ channels ($l=1, 2$) are several orders of magnitude smaller than the ones in the α channels, one has $\det(1 + i\mu\mathcal{H}) \approx 1 + i\mu_{l\alpha}\mathcal{H}_{l\alpha\alpha}$, so that it suffices to take²²

$$\mathcal{T}_{l\gamma\alpha} = 2ip_{l\gamma}p_{l\alpha}\mathcal{H}_{l\gamma\alpha}/(1 + i\mu_{l\alpha}\mathcal{H}_{l\alpha\alpha}), \quad (3.2)$$

and similarly for the matrix element corresponding to the elastic scattering

$$\mathcal{T}_{l\alpha\alpha} = 2ip_{l\alpha}^2\mathcal{H}_{l\alpha\alpha}/(1 + i\mu_{l\alpha}\mathcal{H}_{l\alpha\alpha}), \quad (3.3)$$

and to verify *a posteriori* that it is indeed justified to use these approximations. The phase shift corresponding to the latter equation is then

$$\delta_l = \arctan(-\mu_{l\alpha}\mathcal{H}_{l\alpha\alpha}). \quad (3.4)$$

In the energy range of interest, we will assume a two-level approximation plus background for $\mathcal{H}_{l\gamma\alpha}$ and $\mathcal{H}_{l\alpha\alpha}$, namely

$$\mathcal{H}_{l\gamma\alpha} = \frac{g_{l\gamma 1}g_{l\alpha 1}}{E - E_{l1}} + \frac{g_{l\gamma 2}g_{l\alpha 2}}{E - E_{l2}} + B_{l\gamma\alpha}, \quad (3.5)$$

$$\mathcal{H}_{l\alpha\alpha} = \frac{g_{l\alpha 1}^2}{E - E_{l1}} + \frac{g_{l\alpha 2}^2}{E - E_{l2}} + B_{l\alpha\alpha}. \quad (3.6)$$

As seen in Fig. 1 and Ref. 33, for $l=1$, the two 1^- states are $E_{11} = -0.0451$ MeV and $E_{12} \approx 2.44$ MeV. The bound-state energy E_{11} will not be a free parameter. The corresponding reduced γ width $g_{1\gamma 1}^2$ can also be fixed *a priori* by Eqs. (2.5) and (2.6) and the experimental value of the partial width $\Gamma_{1\gamma 1}$ at $E = E_{11}$, namely³³

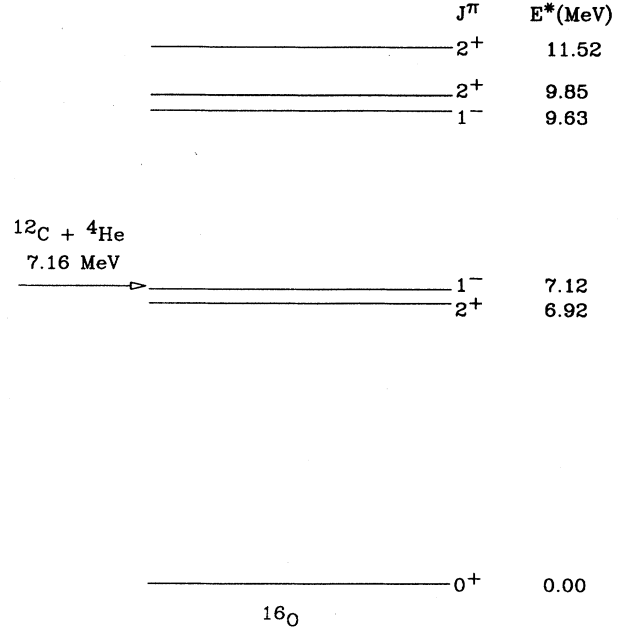


FIG. 1. Energy levels of ^{16}O entering into the present analysis of the $^{12}\text{C}(\alpha, \gamma)^{16}\text{O}$ and $^{12}\text{C}(\alpha, \alpha)^{12}\text{C}$ data.

$$2g_{1\gamma 1}^2(p_{1\gamma}^2)_{E=E_{11}} = (\Gamma_{1\gamma 1})_{E=E_{11}} = 0.055 \pm 0.003 \text{ eV} \quad (3.7)$$

with

$$p_{1\gamma}^2 = k_\gamma^3 = [(7.16195 + E)/\hbar c]^3. \quad (3.8)$$

In Ref. 22, the data of Dyer and Barnes¹⁶ have been fitted up to 3 MeV for σ_{E1} and those of Jones *et al.*²⁶ up to 3.2 MeV for δ_1 , with constant backgrounds $B_{l\gamma\alpha}, B_{l\alpha\alpha}$. Such a fit mainly covers the range of the broad E_{12} resonance and has little sensitivity to the background terms. Moreover, just above 3.2 MeV the parametrized δ_1 is strongly increasing. This behavior is inconsistent with the data recently obtained by Plaga *et al.*³ showing that δ_1 decreases at $E > 3.34$ MeV. Because of this we are extending the fitting of δ_1 up to 4.3 MeV in order to better constrain the free parameters. However, this can only be done by departing from constant background terms. We do this by introducing an echo pole into the backgrounds

$$B_{l\gamma\alpha} = b_{l\gamma\alpha} + \frac{g_{l\gamma 3}g_{l\alpha 3}}{E - E_{13}}, \quad (3.9a)$$

$$B_{l\alpha\alpha} = b_{l\alpha\alpha} + \frac{g_{l\alpha 3}^2}{E - E_{13}}, \quad (3.9b)$$

where the parameters $b_{l\gamma\alpha}, b_{l\alpha\alpha}$ are real, while $g_{l\gamma 3}, g_{l\alpha 3}$ are imaginary. From Eqs. (3.4), (3.6), and (3.9b), we have

$$\frac{d\delta_l}{dE} \bigg|_{E=E_{l\lambda}} = \frac{1}{p_{l\alpha}^2(E_{l\lambda})g_{l\alpha\lambda}^2} \quad (3.10)$$

so that the phase $\delta_1(E)$ is increasing through $\pi/2$ at

$E = E_{12}$, but decreasing through $\pi/2$ at $E = E_{13}$ since $g_{1\alpha 3}^2 < 0$. The data have not been obtained at energies large enough to allow a precise and direct determination of E_{13} , therefore we took $E_{13} = 7$ MeV as a fixed parameter.³⁴ One should note however that a good fit to the σ_{E1} and δ_1 data, in the same energy ranges, is also possible with linear background terms. This is discussed in Sec. VI.

For $l=2$, we can disregard the very narrow 2^+ state at 2.683 MeV for reasons explained in Sec. V, so that the only two states entering into the resonance terms of $\mathcal{H}_{2\gamma\alpha}$ and $\mathcal{H}_{2\alpha\alpha}$ are

$$\begin{aligned} E_{21} &= -0.2448 \pm 0.0006 \text{ MeV} , \\ E_{22} &= 4.358 \pm 0.004 \text{ MeV} . \end{aligned} \quad (3.11)$$

These energies are also measured quantities and the corresponding partial γ widths have been obtained by independent experimental data.^{33,35} They are

$$\begin{aligned} (\Gamma_{2\gamma 1})_{E=E_{21}} &= 0.097 \pm 0.003 \text{ eV} , \\ (\Gamma_{2\gamma 2})_{E=E_{22}} &= 0.61 \pm 0.02 \text{ eV} . \end{aligned} \quad (3.12)$$

Here, $\Gamma_{2\gamma\lambda} = 2g_{2\gamma\lambda}^2 k_\gamma^5$, and E_{21} as well as $g_{2\gamma 1}^2$ will be fixed *a priori*. As for E_{22} , since the phase shift δ_2 is very sensitive to its value, we allowed it to vary within the range of its experimental error.

In view of fitting σ_{E2} and δ_2 , respectively, up to 2.5 and 4.92 MeV, we first adopted background terms similar to those we took for $l=1$, namely

$$B_{2\gamma\alpha} = b_{2\gamma\alpha} + \frac{g_{2\gamma 3} g_{2\alpha 3}}{E - E_{23}} , \quad (3.13a)$$

$$B_{2\alpha\alpha} = b_{2\alpha\alpha} + \frac{g_{2\alpha 3}^2}{E - E_{23}} , \quad (3.13b)$$

where the free parameters $b_{2\gamma\alpha}, b_{2\alpha\alpha}$ are real and $g_{2\gamma 3}, g_{2\alpha 3}$ imaginary, while $E_{23} = 8$ MeV is a fixed parameter.³⁶ But, as δ_2 has not yet reached a maximum at 4.92 MeV, we have also made an alternative parametrization with linear background terms (see Sec. VI).

IV. FITTING σ_{E1} AND δ_1

The presently available data on σ_{E1} are still limited to energies not exceeding 3 MeV, as in the \mathcal{H} -matrix parametrization reported in Ref. 22. But, in order to constrain the background contributions better, we have now fitted δ_1 up to 4.3 MeV. The background terms given by Eqs. (3.9) seem best adapted to fit the behavior of δ_1 both at low and higher energies. In all, with eight free parameters, namely

$$g_{1\alpha 1}, E_{12}, g_{1\alpha 2}, g_{1\gamma 2}, g_{1\alpha 3}, g_{1\gamma 3}, b_{1\alpha\alpha}, b_{1\gamma\alpha} , \quad (4.1)$$

we have fitted *simultaneously* the $^{12}\text{C}(\alpha, \gamma)^{16}\text{O}$ data and the phase shift. For the latter we combined the data of Clark *et al.*,²⁵ Jones *et al.*,²⁶ and Plaga *et al.*³ For reasons discussed below, the $E1$ capture data of Dyer and Barnes,¹⁶ Redder *et al.*² and the new Caltech⁴ data have been analyzed *separately*. For the phase-shift data, we have removed a data point from the Plaga *et al.*³ data set at $E_{\text{c.m.}} = 2.68$ MeV because of its large contributions to the minimized χ^2 in our initial fits. This point corresponds to the location of the 2^+ resonance which appears to be systematically affecting the extracted value of the $E1$ phase shift at this energy. In addition, we have removed some data points where there is a large concentration of data points in a narrow range of energies, so as not to bias the fits to a particular energy range.

There are many more data points for the elastic scattering than for the capture measurements (i.e., $N_{\alpha\alpha} \gg N_{\alpha\gamma}$) and the former ones have smaller error bars

TABLE I. Numerical results of the fit to the $E1$ capture and scattering data with an echo pole in the background terms of the \mathcal{H} matrix. Numbers in parentheses have been obtained from earlier works and are fixed parameters in the present analysis.

	Dyer and Barnes	Data Redder <i>et al.</i>	New Caltech
E_{11} (MeV)	(-0.0451)	(-0.0451)	(-0.0451)
$g_{1\alpha 1} a^{-3/2}$ (MeV ^{1/2})	-0.926	-4.20	-3.70
$g_{1\gamma 1} a^{-3/2}$ (MeV ^{1/2})	(1.897×10^{-3})	(1.897×10^{-3})	(1.897×10^{-3})
E_{12} (MeV)	2.449	2.451	2.449
$g_{1\alpha 2} a^{-3/2}$ (MeV ^{1/2})	7.11	7.08	7.08
$g_{1\gamma 2} a^{-3/2}$ (MeV ^{1/2})	0.639×10^{-3}	0.652×10^{-3}	0.651×10^{-3}
E_{13} (MeV)	(7.000)	(7.000)	(7.000)
$g_{1\alpha 3} a^{-3/2}$ (MeV ^{1/2})	10.9i	11.4i	11.1i
$g_{1\gamma 3} a^{-3/2}$ (MeV ^{1/2})	$8.00 \times 10^{-3}i$	$6.59 \times 10^{-3}i$	$-0.767 \times 10^{-3}i$
$b_{1\alpha\alpha} a^{-3}$	-55.6	-63.4	-60.1
$b_{1\gamma\alpha} a^{-3}$	-23.3×10^{-3}	-18.8×10^{-3}	-0.770×10^{-3}
$\Gamma_{1\gamma 1}$ (MeV)	(55×10^{-9})	(55×10^{-9})	(55×10^{-9})
$\Gamma_{1\alpha 2}$ (MeV)	0.459	0.456	0.454
$\Gamma_{1\gamma 2}$ (MeV)	15.4×10^{-9}	16.0×10^{-9}	15.9×10^{-9}
$S_{E1}(03)$ (MeV b) at χ_{\min}^2	0.014	0.050	0.028
Range $S_{E1}(0.3)$ (MeV b)	0.00-0.16	0.00-0.19	0.00-0.15

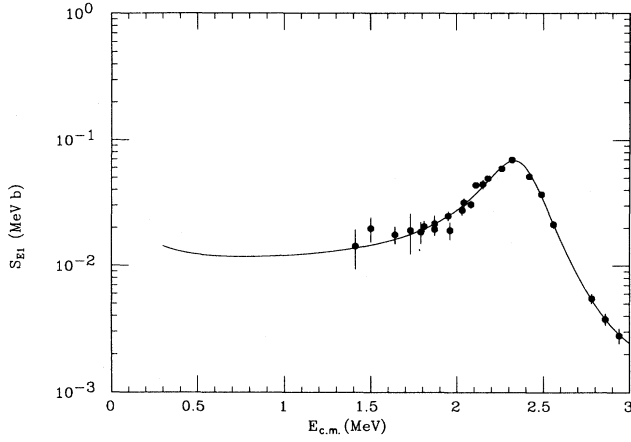


FIG. 2. \mathcal{H} -matrix fit to the $E1$ capture data of Dyer and Barnes (Ref. 16) with two levels and one echo pole when the phase shift δ_1 is simultaneously fitted.

than the latter ones. But, since we are primarily interested in obtaining the best possible parametrization for the (α, γ) cross section, we want to use these two sets of data in such a way that the (α, γ) data should not be given less weight than the (α, α) data. To this end, we first minimized an *ad hoc* effective χ^2 defined as

$$\chi_{\text{eff}}^2 = \frac{1}{2} \left[\frac{\chi_{\alpha\gamma}^2}{N_{\alpha\gamma}} + \frac{\chi_{\alpha\alpha}^2}{N_{\alpha\alpha}} \right]. \quad (4.2)$$

However, after also minimizing the conventional

$$\chi_v^2 = \frac{\chi_{\alpha\gamma}^2 + \chi_{\alpha\alpha}^2}{N_{\alpha\gamma} + N_{\alpha\alpha} - 8}, \quad (4.3)$$

we observed that the two “best sets” of parameters we had obtained were very nearly the same, and fitted the data with a nearly equal quality.

The eight free parameters are all independent of any channel radius, as is the \mathcal{H} matrix itself. But, as seen from Eqs. (2.1)–(2.3), the \mathcal{H} matrix is not dimensionless,

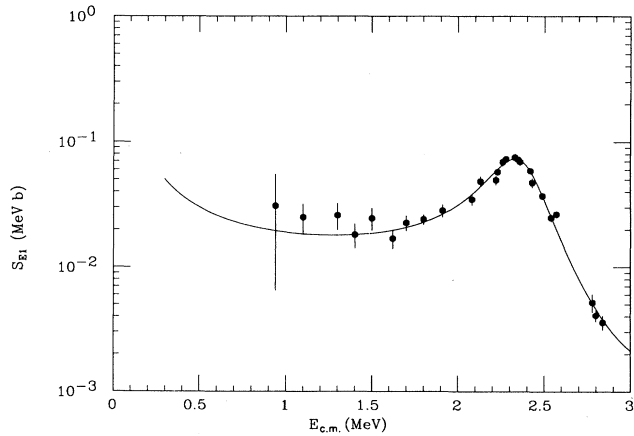


FIG. 3. \mathcal{H} -matrix fit to the $E1$ capture data of Redder *et al.* (Ref. 2) under the same conditions as in Fig. 2.

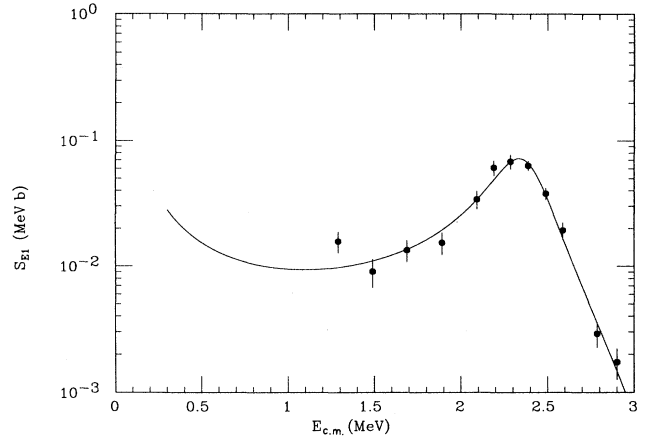


FIG. 4. \mathcal{H} -matrix fit to the $E1$ capture data of Kremer *et al.* (Ref. 4) under the same conditions as in Fig. 2.

so that its residues and background terms do not have their usual dimensions. For that reason, in Table I, as in Ref. 22, we give the numerical values of the g and b multiplied by $a^{-3/2}$ and a^{-3} , respectively, with $a = 5.46$ fm. This leaves the partial width unaffected, of course. The values of $S_{E1}(0.3)$ which minimize χ_{eff}^2 , at $\chi_{\text{eff}}^2 = \chi_{\text{min}}^2$, are, respectively,

$$\begin{aligned} S_{E1}(0.3) &= 0.014 \text{ with } \chi_{\text{min}}^2 = 1.20 \text{ and } \chi_{\alpha\gamma}^2/N_{\alpha\gamma} = 1.10 \\ &= 0.050 \text{ with } \chi_{\text{min}}^2 = 1.46 \text{ and } \chi_{\alpha\gamma}^2/N_{\alpha\gamma} = 1.53 \\ &= 0.028 \text{ with } \chi_{\text{min}}^2 = 1.13 \text{ and } \chi_{\alpha\gamma}^2/N_{\alpha\gamma} = 0.92 \end{aligned} \quad (4.4)$$

for the three sets of data (always given in chronological order: Dyer and Barnes,¹⁶ Redder *et al.*,² and the new Caltech⁴ data). The best fits to the σ_{E1} data are illustrated in Figs. 2–4 in the form of S_{E1} factors. As the three fits to the δ_1 data are hardly distinguishable, we show, in Fig. 5, only the one obtained when the new Caltech⁴ data

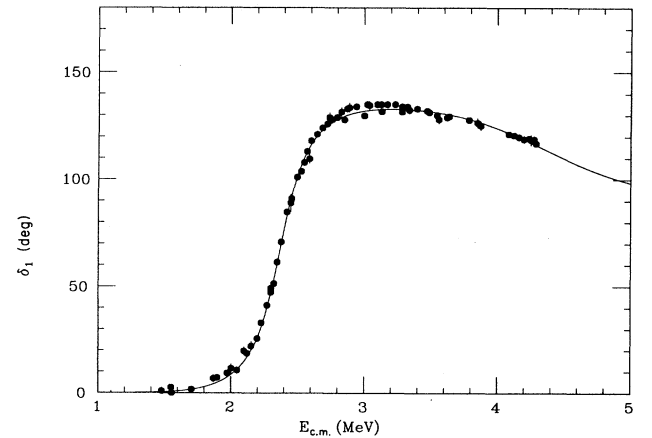


FIG. 5. \mathcal{H} -matrix fit to the δ_1 phase-shift data for $^{12}\text{C}(\alpha, \alpha)^{12}\text{C}$ obtained when the new Caltech (Ref. 4) capture data are simultaneously fitted, as shown in Fig. 4.

for the $E1$ capture are simultaneously fitted. The parameters corresponding to the best fits are all given in Table I.

It has been observed previously^{16,22} that, in the fits to obtain $S_{E1}(E)$, the fitted reduced α width of the bound state is strongly correlated with the background term. Here, in $\mathcal{H}_{1\gamma\alpha}$, we also observed that $g_{1\alpha1}$ is strongly correlated with $b_{1\gamma\alpha}$. In order to determine the uncertainty in $S_{E1}(0.3)$ without concern of this correlation, we eliminated $g_{1\alpha1}$ from σ_{E1} and δ_1 , and replaced it by $S_{E1}(0.3)$. This is possible because $|\mu_{1\alpha}\mathcal{H}_{1\alpha\alpha}| \sim 10^{-11}$ at $E=0.3$ MeV so that, from Eqs. (1.1), (3.1), and (3.2), we obtain

$$S_{E1}(0.3)^{1/2} = -4.1836 \times 10^{-2} \mathcal{H}_{1\gamma\alpha}(0.3) (\text{MeV b})^{1/2} \quad (4.5)$$

and

$$g_{1\alpha1} = \left[\frac{S_{E1}(0.3)^{1/2}}{4.1836 \times 10^{-2}} + \frac{g_{1\gamma2}g_{1\alpha2}}{0.3 - E_{12}} + \frac{g_{1\gamma3}g_{1\alpha3}}{0.3 - E_{13}} + b_{1\gamma\alpha} \right] \frac{E_{11} - 0.3}{g_{1\gamma1}}. \quad (4.6)$$

Then, for a series of selected values of $S_{E1}(0.3)$ in the range 0.00–0.30 MeV b, we obtained the best simultaneous fit to the measured σ_{E1} and δ_1 while the seven other free parameters were allowed to vary. The results are given in Fig. 6, where we have plotted χ^2_{eff} versus $S_{E1}(0.3)$ for the three sets of data. It is clear that the curves representing χ^2_{eff} are quite flat in the neighborhood of their minimal values. For a 95% confidence level, corresponding to an increase of about 30% of the minimal values of χ^2_{eff} , we obtain the following allowed ranges for $S_{E1}(0.3)$:

$$0.00\text{--}0.16, \quad 0.00\text{--}0.19, \quad 0.00\text{--}0.15 \text{ MeV b} \quad (4.7)$$

for the three sets of data, respectively.

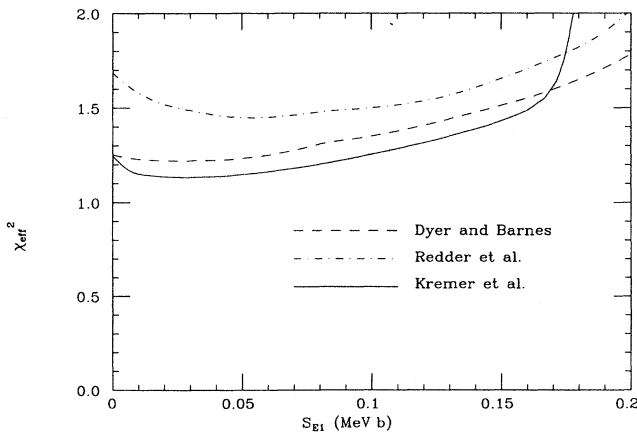


FIG. 6. For each of the three sets of $E1$ capture data, the minimum value of χ^2_{eff} is obtained for a series of fixed values assigned to $S_{E1}(0.3)$, in the range 0.00–0.20 MeV b. From these curves, we extracted the ranges for $S_{E1}(0.3)$ as given by Eq. (4.7).

V. FITTING σ_{E2} AND δ_2

We have fitted the $E2$ capture cross section σ_{E2} to data derived from those given by Redder *et al.*² for the ratio σ_{E2}/σ_{E1} . These authors have obtained three different sets of data for σ_{E2}/σ_{E1} . As their σ_{E1} data and two of the σ_{E2}/σ_{E1} data sets have been measured at different energies, they first averaged their data over 100 keV intervals and then used their σ_{E1} fit to obtain their σ_{E2} data. This procedure may introduce a bias in σ_{E2} as the fit for σ_{E1} is constrained by the data with small uncertainties. In addition, the three sets of data obtained for σ_{E2} are not always mutually compatible.

We proceeded differently. Each measurement of σ_{E2}/σ_{E1} was treated separately. To obtain σ_{E2} at the energies where these ratios have been measured by Redder *et al.*, we made a polynomial interpolation to their *measured* σ_{E1} data. The errors we assigned to these values of σ_{E1} were obtained from the experimental errors of the nearby points; however the errors on σ_{E2} are dominated by the larger errors on the σ_{E2}/σ_{E1} data. By this procedure, we derived three sets of data for σ_{E2} , corresponding to the three sets of data given by Redder *et al.* for σ_{E2}/σ_{E1} . They are shown in Fig. 8.

We then performed χ^2 fits to the combined elastic data of Plaga *et al.*³ for δ_2 and the σ_{E2} data, taking all three sets of Redder *et al.*² together. However, we included only the σ_{E2} data up to $E_{\text{c.m.}} = 2.5$ MeV because, at higher energies, there may be contributions from the narrow 2^+ state at 2.68 MeV ($\Gamma_\alpha = 0.625$ keV). This state has an effective total width of 80 keV in the σ_{E2} data due to the finite target thickness, which might introduce some ambiguities into the \mathcal{H} -matrix analysis. Thus, we neglected all data that might be influenced by this state. Dyer and Barnes¹⁶ have measured σ_{E2}/σ_{E1} at four different energies, but only two of them are below 2.50

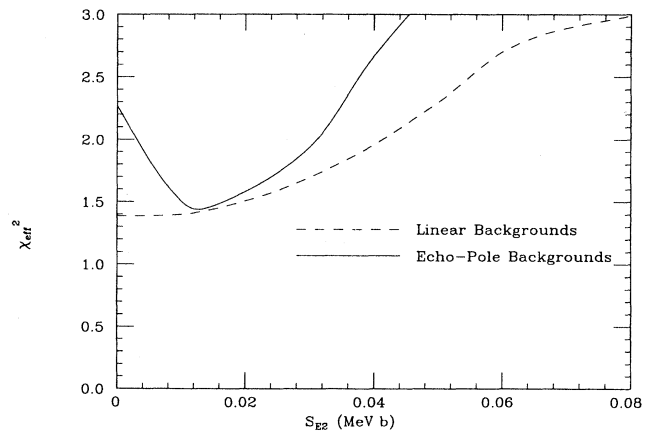


FIG. 7. Two curves similar to those shown in Fig. 6 have been obtained for the $E2$ capture data of Redder *et al.* (Ref. 2). One is obtained with an echo pole in the background terms of \mathcal{H} [Eqs. (3.13)], the other with the linear backgrounds [Eqs. (6.5)]. From these curves, we extracted the ranges for $S_{E2}(0.3)$ as given in Tables II and III.

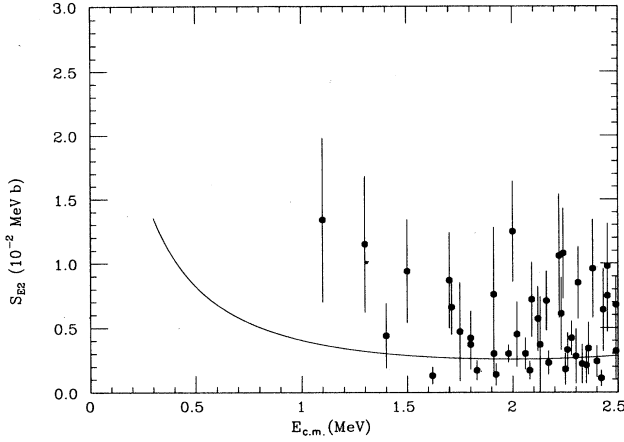


FIG. 8. Fit to the $E2$ capture data of Redder *et al.* (Ref. 2) with two levels and one echo pole when the phase shift δ_2 is simultaneously fitted.

MeV. Because these two data points have considerably larger uncertainties than the Redder *et al.* data, they were not included in our fit.

Because of the relatively thin target used by Plaga *et al.*,³ the narrow 2^+ state at 2.68 MeV seems not to have influenced the δ_2 data. Accordingly, we have not introduced this state in our fit to their data. We fitted the data for δ_2 up to 4.92 MeV in order to constrain the free parameters. According to Sec. III, seven free parameters are available to fit the combined σ_{E2} and δ_2 data, namely

$$g_{2\alpha 1}, E_{22}, g_{2\alpha 2}, g_{2\alpha 3}, g_{2\gamma 3}, b_{2\alpha\alpha}, b_{2\gamma\alpha}. \quad (5.1)$$

In order to evaluate the uncertainty in the S_{E2} factor at 0.3 MeV, we rewrote the elements of the parametrized \mathcal{H} matrix introducing $S_{E2}(0.3)$ rather than $g_{2\alpha 1}$ as a free parameter. This was done as in Sec. IV, now using the relation

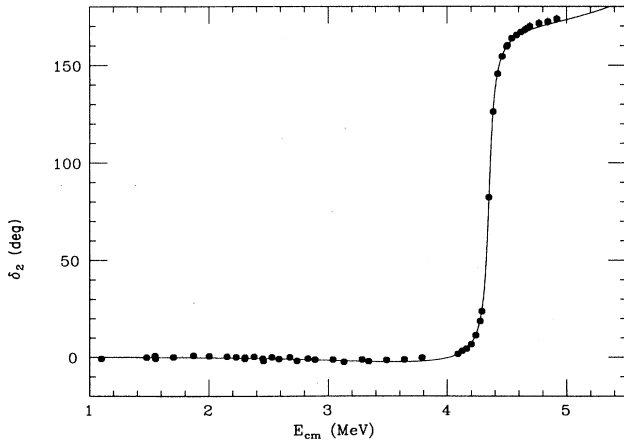


FIG. 9. Fit to the δ_2 phase-shift data of Plaga *et al.*³ for $^{12}\text{C}(\alpha, \alpha)^{12}\text{C}$ obtained when the capture data in Fig. 8 are simultaneously fitted.

TABLE II. Numerical results of the fit to the $E2$ capture and scattering data with an echo pole in the background terms of the \mathcal{H} matrix.

E_{21} (MeV)	(-0.245)
$g_{2\alpha 1}a^{-5/2}$ (MeV $^{1/2}$)	-0.802
$g_{2\gamma 1}a^{-5/2}$ (MeV $^{1/2}$)	(13.7×10^{-3})
E_{22} (MeV)	4.355
$g_{2\alpha 2}a^{-5/2}$ (MeV $^{1/2}$)	94.7×10^{-3}
$g_{2\gamma 2}a^{-5/2}$ (MeV $^{1/2}$)	(9.63×10^{-3})
E_{23} (MeV)	(8.000)
$g_{2\alpha 3}a^{-5/2}$ (MeV $^{1/2}$)	0.0770i
$g_{2\gamma 3}a^{-5/2}$ (MeV $^{1/2}$)	-0.259i
$b_{2\alpha\alpha}a^{-5}$	-0.126
$b_{2\gamma\alpha}a^{-5}$	5.15×10^{-3}
$\Gamma_{2\gamma 1}$ (eV)	(0.097)
$\Gamma_{2\alpha 2}$ (MeV)	0.078
$\Gamma_{2\gamma 2}$ (MeV)	(0.61)
$S_{E2}(0.3)$ (MeV b) at χ^2_{\min}	0.014
$S_{E2}(0.3)$ (MeV b) range	0.005–0.028

$$S_{E2}(0.3)^{1/2} = -1.3357 \times 10^{-3} \mathcal{H}_{2\gamma\alpha}(0.3)(\text{MeV b})^{1/2}. \quad (5.2)$$

We obtained χ^2_{eff} for fixed values of $S_{E2}(0.3)$ in the range 0.00–0.15 MeV b, each time allowing the other six parameters to vary. The results are shown in Fig. 7. At $\chi^2_{\text{eff}} = \chi^2_{\min} = 1.43$, we have $S_{E2}(0.3) = 0.014$ MeV b, $\chi^2_v = 1.50$, $\chi^2_{\alpha\gamma}/N_{\alpha\gamma} = 1.93$, $\chi^2_{\alpha\alpha}/N_{\alpha\alpha} = 0.93$ and the corresponding fits are shown in Figs. 8 and 9. Table II gives the values of the various parameters. For a 95% confidence level, corresponding to an increase of about 30% of the minimal value of χ^2_{eff} , we obtain from Fig. 7 the range 0.005–0.028 for the S_{E2} factor at 0.3 MeV.

VI. DISCUSSION AND CONCLUSION

Considering first the $E1$ capture, Table I suggests for the astrophysical factor

$$S_{E1}(0.3) = 0.03^{+0.14}_{-0.03} \text{ MeV b}, \quad (6.1)$$

which corresponds to the average of the three sets of results reported in that table.

Two of the three values of $S_{E1}(0.3)$ at χ^2_{\min} differ by as much as a factor of 3.6, while the three ranges differ by no more than 13 % from their average. Therefore, we must stress that the main result of our analysis is that, from the presently available data, one can deduce for $S_{E1}(0.3)$ a range of acceptable values, namely 0.00–0.17 MeV b, rather than a reliable best value. This point of view was already stressed as a result of the two R -matrix analyses reported in Ref. 4. It is also suggested by other \mathcal{H} -matrix parametrizations briefly discussed below.

The parameters of the broad resonance ($E_{12}, g_{1\alpha 2}, g_{1\gamma 2}$) are well determined and they are nearly the same for the three sets of data. But the situation is very different for $g_{1\alpha 1}$ associated with the bound state. With an R -matrix parametrization, Dyer and Barnes¹⁶ observed that the reduced α width of that state is strongly correlated with the background term, and this has been confirmed by the R -

matrix analysis of the new Caltech data.⁴ If the reduced α width of the bound state is given a fixed value different from its “best” one, one can still obtain a good fit of the data if the background terms are modified accordingly. The same situation prevails in the present \mathcal{H} -matrix parametrization, since it is obviously related to the fact that no data have been obtained below $\simeq 1$ MeV for σ_{E1} and below 1.45 MeV for δ_1 , while only δ_1 has been measured above 3 MeV.

Under such conditions, we must also expect that the values reported in Table I for $g_{1\alpha 1}$ and $S_{E1}(0.3)$ are to some extent linked to the type of energy dependence adopted in this analysis for the background terms, namely a constant plus an echo pole. This is indeed the case, since with linear backgrounds

$$B_{1\gamma\alpha} = b_{1\gamma\alpha} + Eb'_{1\gamma\alpha}, \quad (6.2a)$$

$$B_{1\alpha\alpha} = b_{1\alpha\alpha} + Eb'_{1\alpha\alpha}, \quad (6.2b)$$

where the b, b' are constant free parameters, we have obtained the following results from the three sets of data, respectively:

$$\begin{aligned} \chi_{\min}^2 &= 1.10, 1.25, 1.01, \\ g_{1\alpha 1} a^{-3/2} &= -0.962, -5.95, -6.02 \text{ MeV}^{1/2}, \\ S_{E1}(0.3) &= 0.018, 0.079, 0.051 \text{ MeV b}, \end{aligned} \quad (6.3)$$

$$\begin{aligned} S_{E1}(0.3) \text{ range} \\ &= 0.00-0.25, 0.00-0.29, 0.00-0.18 \text{ MeV b}. \end{aligned}$$

Taking $b'_{1\gamma\alpha} = 0$ *a priori* does not increase χ_{\min}^2 significantly, but the parameters are changed considerably. We obtained

$$\begin{aligned} \chi_{\min}^2 &= 1.23, 1.33, 1.03, \\ g_{1\alpha 1} a^{-3/2} &= -10.0, -10.6, -3.05 \text{ MeV}^{1/2}, \\ S_{E1}(0.3) &= 0.14, 0.16, 0.023 \text{ MeV b}, \end{aligned} \quad (6.4)$$

$$\begin{aligned} S_{E1}(0.3) \text{ range} \\ &= 0.04-0.27, 0.05-0.28, 0.00-0.09 \text{ MeV b}. \end{aligned}$$

With $b'_{1\gamma\alpha} = b'_{1\alpha\alpha} = 0$, in Ref. 22, $g_{1\alpha 1} a^{-3/2} = -7.15 \text{ MeV}^{1/2}$ was obtained. In contrast with $g_{1\alpha 1}$, the parameters of the E_{12} resonance, $g_{1\gamma 2}$ and $g_{1\alpha 2}$, are hardly modified by the linear backgrounds (6.2). Note that, in the calculations of Barker,^{12,37} the contribution from a background level is set to zero for the capture channel. For the present calculation, this would amount to taking $b_{1\gamma\alpha} = g_{1\gamma 3} = 0$ and $b_{1\gamma\alpha} = b'_{1\gamma\alpha} = 0$, respectively, for the two types of backgrounds we have adopted. Barker's assumption is based on model-dependent shell-model arguments. However, these arguments do not warrant complete neglect of a background contribution, as there are experimentally observed states in ^{16}O with higher excitation that could, in principle, contribute.

The results (6.3), (6.4), and those given in Sec. IV show clearly that, for each set of data, the values of $S_{E1}(0.3)$ at χ_{\min}^2 are indeed correlated with the analytical form given to the background terms of the \mathcal{H} -matrix elements.

We have not included the two parametrizations (6.3) and (6.4) into the average values (6.1) because, *a priori*, the echo pole allows a more physically reasonable parametrization of δ_1 above 3 MeV. With the linear backgrounds (6.2), δ_1 is constrained to remain between $\pi/2$ and $3\pi/2$ above 3 MeV.

The three sets of $E1$ radiative capture data lead to rather large differences in the results (6.3) and (6.4), and in Table I. This suggests that there may be significant differences between the three data sets. This is confirmed by the fact that a simultaneous fit of the three sets of data have a much larger χ_{\min}^2 than those given by Eqs. (4.4).

The data for the phase shift δ_2 have been fitted over the range 1.1–4.92 MeV. But those for the $E2$ capture are limited to the range 1.1–2.5 MeV, i.e., a much shorter range well below the energy of the echo pole E_{23} fixed at 8 MeV. This can explain why, in Table II, $g_{2\gamma 3}$ is unexpectedly large. In analogy with the $E1$ capture, we expected $|g_{2\gamma 3}/g_{2\alpha 3}| \ll 1$, rather than $|g_{2\gamma 3}/g_{2\alpha 3}| = 3.36$ as seen from Table II. For that reason, as well as to estimate the correlation between the analytical form of the background terms and the free parameters $g_{2\alpha 1}$ and $g_{2\alpha 2}$, we also fitted the data to linear backgrounds, i.e., by taking

$$B_{2\gamma\alpha} = b_{2\gamma\alpha} + Eb'_{2\gamma\alpha}, \quad (6.5a)$$

$$B_{2\alpha\alpha} = b_{2\alpha\alpha} + Eb'_{2\alpha\alpha}, \quad (6.5b)$$

the total number of free parameters remaining unchanged. χ_{eff}^2 has been minimized at $\chi_{\min}^2 = 1.39$, and we obtained the results reported in Table III. The correlation with the background terms is, as expected, important for $g_{2\alpha 1}$ and negligible for $g_{2\alpha 2}$, while the two ratios $|b_{2\gamma\alpha}/b_{2\alpha\alpha}|, |b'_{2\gamma\alpha}/b'_{2\alpha\alpha}|$, are now of the order of $\frac{1}{10}$. Since the measured δ_2 is still increasing at 4.92 MeV, we cannot disregard this linear parametrization (6.5) and retain only the one with an echo pole (3.16) at $E_{23} = 8$ MeV. As shown in Fig. 7, the curve giving χ_{eff}^2 versus $S_{E2}(0.3)$ is lower than the one obtained with linear backgrounds. We have also fitted the same data to quadratic back-

TABLE III. Numerical results of the fit to the $E2$ capture and scattering data with linear background terms of the \mathcal{H} matrix.

E_{21} (MeV)	(-0.245)
$g_{2\alpha 1} a^{-5/2}$ (MeV ^{1/2})	0.369
$g_{2\gamma 1} a^{-5/2}$ (MeV ^{1/2})	(13.7×10^{-3})
E_{22} (MeV)	4.355
$g_{2\alpha 2} a^{-5/2}$ (MeV ^{1/2})	9.49×10^{-2}
$g_{2\gamma 2} a^{-5/2}$ (MeV ^{1/2})	(9.63×10^{-3})
$b_{2\alpha\alpha} a^{-5}$	-9.99×10^{-2}
$b'_{2\alpha\alpha} a^{-5}$ (MeV ⁻¹)	2.60×10^{-2}
$b_{2\gamma\alpha} a^{-5}$	1.01×10^{-2}
$b'_{2\gamma\alpha} a^{-5}$ (MeV ⁻¹)	-2.33×10^{-3}
$\Gamma_{2\gamma 1}$ (eV)	(0.097)
$\Gamma_{2\alpha 2}$ (MeV)	0.078
$\Gamma_{2\gamma 2}$ (MeV)	(0.61)
$S_{E2}(0.3)$ (MeV b) at χ_{\min}^2	4.0×10^{-6}
$S_{E2}(0.3)$ (MeV b) range	0.000–0.034

grounds, adding, respectively, $E^2 b''_{2\gamma\alpha}$ and $E^2 b''_{2\alpha\alpha}$ to the right-hand side of Eqs. (6.5a) and (6.5b). In this case, the curve giving χ^2_{eff} versus $S_{E2}(0.3)$ is still lower, but it remains very flat over a broad range (0.00–0.16) including its minimum at $\chi^2_{\text{min}} = 1.33$. This most likely occurs because of the inclusion of the two additional parameters.

Adopting for best value and range of $S_{E2}(0.3)$ the average of the results reported in Tables II and III and corresponding, respectively, to the echo pole and linear backgrounds, we have

$$S_{E2}(0.3) = 0.007^{+0.024}_{-0.005} \text{ MeV b} . \quad (6.6)$$

With the upper limits for $S_{E1}(0.3)$ and $S_{E2}(0.3)$ assumed to be uncorrelated, the latter result (6.6) brings a negligible contribution to the range of the total S factor at 0.3 MeV, and we have

$$S(0.3) = 0.04^{+0.13}_{-0.04} \text{ MeV b} . \quad (6.7)$$

But, here again, we must stress that the main and most reliable result the \mathcal{H} -matrix parametrization can derive

from the present data is the range of acceptable values for $S(0.3)$, namely

$$0.00\text{--}0.17 \text{ MeV b} . \quad (6.8)$$

This range might be even larger if other physically less motivated forms than the echo pole terms, as seen when the ranges in Eq. (6.3) are compared to those in Table I. Consequently, we recommend that astrophysical computations use several S factors within the above range.

ACKNOWLEDGMENTS

The authors are grateful to C. A. Barnes, William A. Fowler, S. E. Koonin, and C. Rolfs for useful discussions. One of us (J.H.) acknowledges support from the “Belgian Fond National de la Recherche Scientifique” and B.W.F. from the Sloan Research Foundation. This work was supported in part by the National Science Foundation, Grant Nos. PHY85-05682 and PHY86-04197.

*Permanent address: Université de Liège, Institut de Physique B5, Sart Tilman, B-4000 Liège 1, Belgium.

†Permanent address: Institut für Theoretische Physik I, Universität Münster, D-4400 Münster, Germany.

¹K. U. Kettner, H. W. Becker, L. Buchmann, J. Görres, H. Krawinkel, C. Rolfs, P. Schmalbrock, H. P. Trautvetter, and A. Vlieks, *Z. Phys. A* **308**, 73 (1982).

²A. Redder, H. W. Becker, C. Rolfs, H. P. Trautvetter, T. R. Donoghue, T. C. Rinckel, J. W. Hammer, and K. Langanke, *Nucl. Phys. A* **462**, 385 (1987).

³R. Plaga, H. W. Becker, A. Redder, C. Rolfs, H. P. Trautvetter, and K. Langanke, *Nucl. Phys. A* **465**, 291 (1987).

⁴R. M. Kremer, C. A. Barnes, K. H. Chang, H. C. Evans, B. W. Filippone, K. H. Hahn, and L. W. Mitchell, *Phys. Rev. Lett.* **60**, 1475 (1988).

⁵K. Langanke and S. E. Koonin, *Nucl. Phys. A* **410**, 334 (1983); **A439**, 384 (1985).

⁶P. Descouvemont, D. Baye, and P.-H. Heenen, *Nucl. Phys. A* **430**, 426 (1984).

⁷C. Funck, K. Langanke, and A. Weiguny, *Phys. Lett.* **152B**, 11 (1985).

⁸P. Descouvemont and D. Baye, *Phys. Rev. C* **36**, 1249 (1987).

⁹W. D. Arnett and F.-K. Thielemann, *Astrophys. J.* **295**, 589 (1985).

¹⁰F.-K. Thielemann and W. D. Arnett, *Astrophys. J.* **295**, 604 (1985).

¹¹S. E. Woosley and T. A. Weaver, in *Nucleosynthesis and Its Implications for Nuclear and Particle Physics*, edited by J. Audouze and N. Mathieu (Reidel, Dordrecht, 1986), p. 145.

¹²F. C. Barker, *Aust. J. Phys.* **40**, 25 (1987).

¹³D. C. Weisser, J. F. Morgan, and D. R. Thompson, *Nucl. Phys. A* **235**, 460 (1974).

¹⁴S. E. Koonin, T. A. Tombrello, and G. Fox, *Nucl. Phys. A* **220**, 221 (1974).

¹⁵W. A. Fowler, G. R. Caughlan, and B. A. Zimmerman, *Annu. Rev. Astron. Astrophys.* **13**, 69 (1975).

¹⁶P. Dyer and C. A. Barnes, *Nucl. Phys. A* **233**, 495 (1974).

¹⁷G. R. Caughlan, W. A. Fowler, M. J. Harris, and B. A. Zimmerman, *At. Data Nucl. Data Tables.* **32**, 197 (1985).

¹⁸B. W. Filippone, *Annu. Rev. Nucl. Part. Sci.* **36**, 717 (1986).

¹⁹C. A. Barnes, in *Advances in Nuclear Astrophysics*, Proceedings of the Second IAP Workshop, edited by E. Vangioni-Flam, J. Audouze, M. Casse, J. P. Chieze, and J. Tran Thanh Van (Editions Frontières, Paris, 1986).

²⁰W. A. Fowler, *Rev. Mod. Phys.* **56**, 149 (1984).

²¹C. E. Rolfs and W. S. Rodney, *Cauldrons in the Cosmos: Nuclear Astrophysics* (University of Chicago Press, Chicago, 1988).

²²J. Humblet, P. Dyer, and B. A. Zimmerman, *Nucl. Phys. A* **271**, 210 (1976).

²³The physical interpretation and illustrative examples of “echoes” can be found in several papers by McVoy and collaborators: K. W. McVoy, *Phys. Lett.* **17**, 42 (1965); K. W. McVoy, L. Heller, and M. Bolsterli, *Rev. Mod. Phys.* **39**, 245 (1967); K. W. McVoy, *Ann. Phys. (N.Y.)* **43**, 91 (1967).

²⁴For the association of the echoes to particular poles of the \mathcal{H} matrix, see J. Humblet, *Nucl. Phys. A* **151**, 225 (1970); **A187**, 65 (1972). In the second paper, numerical examples show that echo poles allow a good parametrization of the non-resonant part of the \mathcal{H} matrix.

²⁵G. J. Clark, D. J. Sullivan, and P. B. Treacy, *Nucl. Phys. A* **110**, 481 (1968).

²⁶C. M. Jones, G. C. Phillips, R. W. Harris, and E. H. Beckner, *Nucl. Phys.* **37**, 1 (1962). These data have been corrected for an energy calibration offset. See Refs. 14 and 16.

²⁷A. M. Lane and R. G. Thomas, *Rev. Mod. Phys.* **30**, 257 (1958); **30**, 287 (1958).

²⁸Equation $\mu_c = 0$ holds for a channel with charged fragments only. For neutron channels, see Ref. 22; neutron channels can be disregarded here.

²⁹J. Humblet, *Ann. Phys. (N.Y.)* **155**, 461 (1984). Note that a factor $u_l(\eta)$ is missing on the left-hand side of Eq. (5.34b), so that $u_l \Psi_l$ is entirely in E , while Ψ_l is not when $l \neq 0$.

³⁰J. Humblet (unpublished). Briefly, the fact that the \mathcal{H} matrix has poles at the energies of the bound states results from the very definition of the modified Coulomb function \bar{G}_l used in the definition of \mathcal{H} and given in the appendix of Ref. 22. At

positive energies \bar{G}_l is practically equal to $\epsilon_l k^l G_l$, but at negative energies \bar{G}_l is typically a bound-state function since it decreases exponentially for large r . From Eqs. (A4) and (A7) of the appendix of Ref. 22, at *negative energies*, i.e., when $k = ib$ ($b > 0$) and $i\eta = \beta > 0$, one has

$$\begin{aligned}\bar{G}_l &= \epsilon_l k^l (G_l + iF_l) \\ &= \epsilon_l k^l \mathcal{O}_l \propto W_{\beta, l+1/2}(2br) \\ &\quad \propto \exp[-br - \beta \ln(2br)]\end{aligned}$$

where W is a Whittaker function.

³¹*Handbook of Mathematical Functions*, 7th ed., Natl. Bur. Stand. Appl. Math. Ser. No. 55, edited by M. Abramowitz and I. A. Stegun (U.S. GPO, Washington, D.C., 1968), Eq. (14.6.7).

³²See, A. M. Lane and R. G. Thomas, *Rev. Mod. Phys.* **30**, 273 (1958), Eq. (1.11).

³³F. Ajzenberg-Selove, *Nucl. Phys.* **A460**, 1 (1986).

³⁴We have checked that allowing the echo-pole energy E_{13} to vary hardly improves the quality of the fit. Its adopted fixed value at 7 MeV is suggested by the downward trend of δ_1 beyond 3.34 MeV. For the sake of comparison, let us also note that in an R -matrix parametrization the falling off of the phase shift is mainly due to the so-called hard-sphere scattering phase shift $-\phi_l$, with $\tan \phi_l = F_l/G_l$. For $\eta = 3.273\,624E^{-1/2}$ and $r = 5.46$ fm (hence $\rho = 2.068\,798E^{1/2}$), $\tan(-\phi_l)$ has a first echo pole at $E = 6.15$ MeV for $l = 1$.

³⁵J. C. Bergstrom and I. P. Auer, *Nucl. Phys.* **A215**, 232 (1973).

³⁶For $l = 2$, $\tan(-\phi_l)$ has a first echo pole at $E = 7.74$ MeV.

³⁷F. C. Barker, *Aust. J. Phys.* **24**, 777 (1971).